Chemical Engineering Journal 323 (2017) 455–464

Contents lists available at ScienceDirect

Chemical Engineering Journal

journal homepage: www.elsevier.com/locate/cej

# Investigation on decolorization of biologically pretreated cellulosic ethanol wastewater by electrochemical method

Lili Shan [a], Junfeng Liu [a,1], John J. Ambuchi [a], Yanling Yu [a,b], Linlin Huang [a], Yujie Feng [a,*]

[a] State Key Laboratory of Urban Water Resource and Environment, Harbin Institute of Technology, Harbin, China
[b] School of Chemical Engineering and Technology, Harbin Institute of Technology, Harbin, China

## HIGHLIGHTS

- Electrochemical decolorization was obviously promoted in acidic condition.
- 100% color and 86.5% COD removal were achieved under the optimal conditions.
- ·OH addition to aromatic structures played a primary role in decolorization.
- Removal of color accompanied with humic acid followed a pseudo first-order reaction.

## ARTICLE INFO

*Article history:*
Received 11 January 2017
Received in revised form 20 April 2017
Accepted 25 April 2017
Available online 27 April 2017

*Keywords:*
Cellulosic ethanol wastewater
Biologically treated effluent
Decolorization
Electrochemical oxidation

## ABSTRACT

The biologically pretreated cellulosic ethanol wastewater poses a serious environmental concern because of its refractory and color compounds. The decolorization of electrochemical oxidation using Sb doped Ti/$SnO_2$ electrode for advanced treatment of cellulosic ethanol wastewater under different current density (5–30 mA·cm$^{-2}$), initial pH (3–8.9) and supporting electrolyte (0–0.25 M NaCl) was investigated in this study. Complete decolorization, 8.5% chemical oxygen demand (COD) and 69.1% dissolved organic carbon removal efficiencies were achieved under the optimal conditions (20 mA·cm$^{-2}$, pH 5 and supporting electrolyte of 0.1 M NaCl) after 150 min. The energy consumption required to meet National Discharge Standard (GB 27631-2011) is 93.8 kWh kg COD$^{-1}$. Further investigation revealed that hydroxyl radicals played a primary role in the degradation of organic contaminants, while active chlorine formed from chloride oxidation played a less important role. Direct anodic oxidation and indirect reaction via peroxodisulfate generated from sulfate oxidation could be negligible. The formation of chlorination by-products appeared to be low since the final total Trihalomethanes concentration detected was 263 μg L$^{-1}$, with the detection of chloroform as the main Trihalomethanes.



## 1. Introduction

The production of ethanol from cellulosic materials has attracted global interest due to an abundance of lignocellulosic resources. However, large quantities of wastewater from the production of cellulosic ethanol pose serious environmental concerns because of its quality (high chemical oxygen demand (COD), organic priority contaminants content, biochemical oxygen demand (BOD) and dark color) [1,2]. Physico-chemical and biological methods have been developed to treat such wastewater [2–4]. However, all these processes are either energy-intensive or incomplete on their own. Biological methods, for example, are more efficient in the reduction of COD, but have little effect on color removal, which can become darker because of re-polymerization of coloring compounds [5]. When discharged into water bodies, the color of wastewater creates aesthetic pollution, inhibits photosynthetic activity of aquatic plants and alters water quality, which may become hazardous to human health [2]. Considering these disadvantages, further decolorization of biologically treated effluents using various alternative methods has been carried out. This include flocculation and coagulation, advanced oxidation processes, bacteria and fungi, and membrane technology [2,6,7]. In addition to its attractiveness, the electrochemical oxidation of organic contaminants has been extensively investigated for wastewater treatment [8]. Its advantages are available in the literature [8,9]. Furthermore, its versatility, operational simplicity and no secondary contamination has made it known as an "environmentally friendly technology" [10].

* Corresponding author.
*E-mail addresses:* Richard@hit.edu.cn (J. Liu), yujief@hit.edu.cn (Y. Feng).
[1] Co-corresponding author.

http://dx.doi.org/10.1016/j.cej.2017.04.121
1385-8947/

The electrochemical oxidation of organic contaminants can be performed through two major processes: direct and indirect oxidation [9,11]. The former process destroys the contaminants directly on the anodic surface, while the latter is mediated by hydroxyl radicals (·OH) generated in the electrochemical process. During electrolysis, ·OH as chemisorbed "active oxygen" ($MO_{x+1}$) can participate in electrochemical conversion resulting in partial oxidation of organic contaminants to RO; when ·OH appears as physically adsorbed active oxygen, complete combustion of organic contaminants would occur as in the following equations:

$$R + MO_{x+1} \rightarrow RO + MO_x \quad (1)$$

$$R + MO_x(\cdot OH)_z \rightarrow CO_2 + zH^+ + ze^- + MO_x \quad (2)$$

where R is organic contaminants, z is the number of absorbed ·OH on anode. In addition, peroxide, active chlorine, peroxodisulfate and ozone are other chemical oxidants generated from electrochemical process [9,11].

Electrochemical oxidation decolorized sugar-based ethanol wastewater containing intense color due to the presence of melanoidin [12,13]. The most recent study demonstrates that color-causing compounds strongly correlate with humic acid-like matter [14], which is different from sugar-based ethanol wastewater (melanoidin) [6,7] and starch-based crops (phenolic compounds) [15]. Nevertheless, the application of electrochemical oxidation on ethanol wastewater from cellulosic feedstocks is extremely limited [14].

The electrochemical oxidation of organic compounds in the presence of chloride can lead to the formation of organochlorinated by-products [16,17], which cannot be neglected but should be given attention. Trihalomethanes (THMs) are common and among the most abundant by-products [18,19], which develop in chlorinated water containing organic precursors, such as humic and fulvic acids [20]. For this reason, it is necessary to monitor the formation of THMs after the electrochemical treatment processes.

This study was conducted to assess the decolorization of biologically pretreated cellulosic ethanol wastewater (CEW) and determine the removal mechanisms of electrochemical oxidation process. Sb doped $Ti/SnO_2$ electrode and stainless steel sheet were used as anode and cathode, respectively. To better understand the color removal, the influence of current density, initial pH, and supporting electrolyte were studied in detail. COD, dissolved organic carbon (DOC) and color removal, UV–Vis spectra, excitation–emission matrix (EEM) fluorescence intensity, and the formation of THMs during the electrochemical process were investigated. The energy consumption (Es) met the discharge standard for fermentation alcohol and distilled spirits industry in China (National Discharge Standard (GB 27631-2011)) was also calculated. The results presented herein will provide valuable information for the industrial application of a promising technology for advanced treatment of CEW.

**Table 1**
Characteristics of wastewater used in the experiments.

| Parameter | Unit | CEW |
|---|---|---|
| Chemical oxygen demand (COD) | mg $L^{-1}$ | 644 |
| Biochemical oxygen demand (BOD) | mg $L^{-1}$ | 98 |
| Total organic carbon (TOC) | mg $L^{-1}$ | 268.4 |
| Conductivity | mS $cm^{-1}$ | 6.9 |
| Color | Pt-Co | 2926 |
| Alkalinity | mg $L^{-1}$ | 4016.5 |
| Sulfate | mg $L^{-1}$ | 134.1 |
| pH | | 8.9 |

## 2. Material and methods

### 2.1. Wastewater samples

The raw CEW was obtained from a cellulosic ethanol plant in Northeast China. A two-phase anaerobic and aerobic system was employed for the wastewater treatment in a laboratory scale. The collected effluent of this system was used in this study. Table 1 summarizes the main characteristics of the collected wastewater.

### 2.2. Electrochemical oxidation experiments

The experiments were carried out in a single-compartment electrochemical cell made of glass (effective volume of 200 mL) in galvanostatic electrolysis mode. Schematic diagram of the electrochemical oxidation cell is shown in Fig. 1. Continuous mixing conditions were provided by magnetic stirring in the electrolysis process, and constant stirring rate was maintained over all the experiments. The Sb doped $Ti/SnO_2$ electrode and stainless steel plate with the same surface area of 24 $cm^2$ were used as the anode, and cathode, respectively. Sb doped $Ti/SnO_2$ electrode was prepared by sol-gel method as previously described [21]. The gap

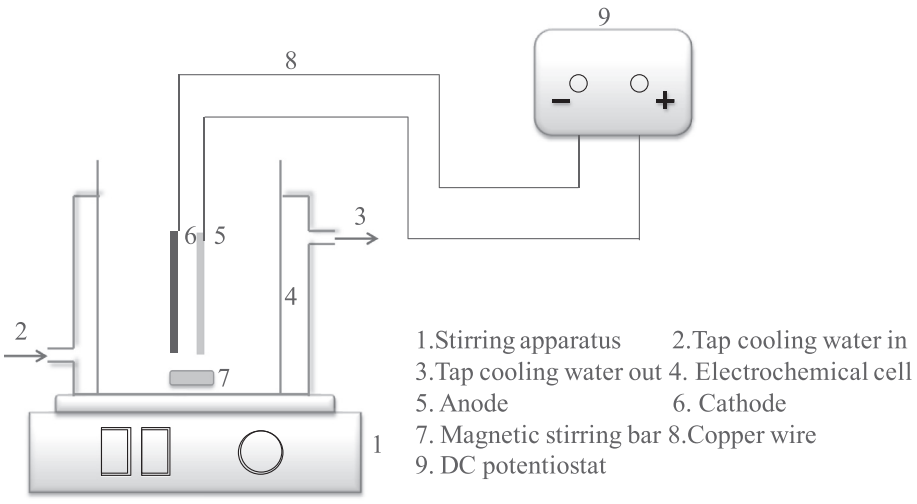


**Fig. 1.** Schematic diagram of the electrochemical oxidation cell.

of anode and cathode was set to be 1 cm. A DC potentiostat with a current output up to 4 A was employed as the power supply. Electrolysis assays were operated at four different current densities (5, 10, 20 and 30 mA·cm$^{-2}$), initial pH (3, 5, 7, not adjusted), and supporting electrolyte (0, 0.01, 0.1 and 0.25 M NaCl). Dilute hydrochloric acid and sodium hydroxide were used to adjust the initial pH. The samples were taken from the electrochemical cell at time 0 min (initial), 5 min, 10 min, 20 min, 30 min, 45 min, 60 min, 90 min, 120 min and 150 min, and filtered through 0.45 μm membrane filters prior to chemical analysis.

### 2.3. Analytical methods

The COD was determined by DRB 200 and DR 3900 spectrophotometer (Hach, USA) at a wavelength of 420 nm. The DOC was measured with a TOC/TN Analyzer (Multi N/C 2100S, AnalytikJena, Germany). A pH meter (inoLab pH 720, WTW, Germany) was used for pH measurements. Color was determined at 465 nm using a Hach DR/3900 spectrophotometer (Hach, USA). UV–Visible spectrophotometer (UV-2550, Shimadzu, Japan) was used to analyze samples in the range of 190–800 nm. Fluorescence EEM measurements were conducted as previously described [14]. Cyclic voltammetry measurements were performed in a three-electrode system comprising of a Sb doped Ti/$SnO_2$ electrode as working electrode, a platinum plate as counter electrode and a saturated calomel electrode (SCE) (saturated KCl, +0.241 V versus standard hydrogen electrode; SHE) as a reference electrode. Trihalomethanes (THMs), which included chloroform ($CHCl_3$), bromodichloromethane ($CHCl_2Br$), dibromochloromethane ($CHClBr_2$) and bromoform ($CHBr_3$), were determined by headspace injection followed by gas chromatography (Agilent-7890 GC, USA) with an electron capture detector (ECD) at 300 °C. A 30 m × 320 μm × 0.25 μm capillary column (HP-5 5% Phenyl Methyl Siloxane, Agilent, USA) was employed. The temperature program was from 45 °C (5 min) to 200 °C (2 min) at 25 °C /min and from 200 °C to 250 °C (2 min) at 15 °C /min. The injector temperature was set at 250 °C.

The Instantaneous Current Efficiency (ICE) from the COD measurements was calculated as follows [9,22]:

$$\%\mathrm{ICE} = \mathrm{FV}\frac{\mathrm{COD}_0 - \mathrm{COD}_t}{8I\Delta t} \times 100 \quad (3)$$

where F is the Faraday constant (96 487 Cmol$^{-1}$), V is the sample volume (L), $COD_0$ and $COD_t$ are the COD concentration (mg L$^{-1}$) measured at the beginning of the experiments and at time t of electrolysis, 8 is the oxygen equivalent mass (g eq$^{-1}$), I is the electrolysis current (A), Δt is the electrolysis time (s).

The energy consumption (Es) required to meet National Discharge Standard (GB 27631-2011) was calculated as follows [23]:

$$\mathrm{Es} = \frac{1000\mathrm{UIt}}{(\mathrm{COD}_0 - \mathrm{COD}_s)\mathrm{V}} \quad (4)$$

where Es is the energy consumption (in kWh kg COD$^{-1}$), U is the average cell voltage (V), I is the electrolysis current (A), t is the time needed to reach the discharge requirement (h), $COD_0$ is the initial COD concentration (mg L$^{-1}$), $CODs$ is 100 mg L$^{-1}$ complied with National Discharge Standard (GB 27631-2011), and V is the sample volume (L).

## 3. Results and discussion

### 3.1. Effect of current density

Electrochemical oxidation of CEW was performed at four different current densities (5, 10, 20 and 30 mA·cm$^{-2}$). Fig. 2a indicates the removal efficiency of color as a function of time at different current densities. As presented in Fig. 2a, the color gradually reduced with increasing current density, and completely disappeared after 150 min of electrolysis at the current density of

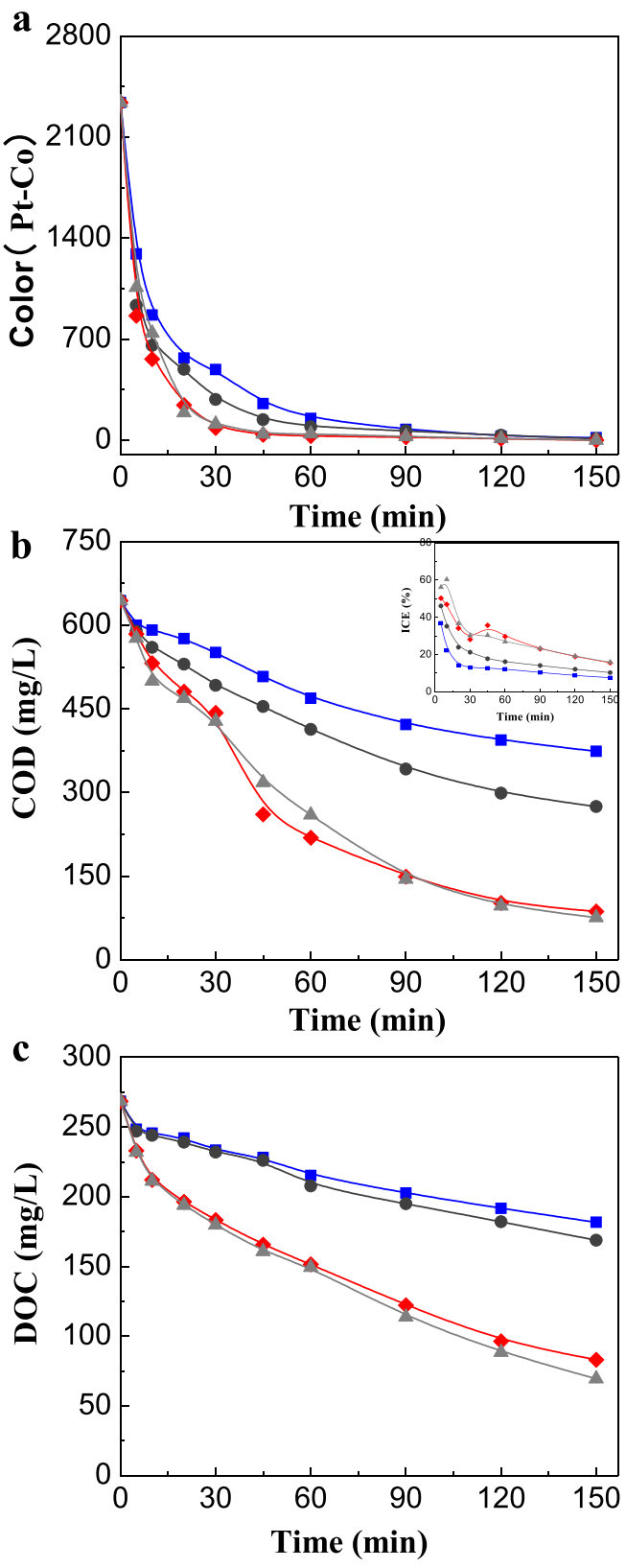


**Fig. 2.** Evolution of Color (a), COD (b) and DOC (c) as a function of time at different current density. Electrolysis conditions: solution (200 mL CEW + 0.1 M NaCl) and pH 5. (a) *Inset*: The instantaneous current efficiency as a function of time. Current density: (■) 5, (●) 10, (◆) 20 and (▲) 30 mA·cm$^{-2}$.

20 mA·cm$^{-2}$. The results show a clear current density effect on the color removal. It has been reported that electrochemical oxidation of contaminants can be performed through direct and indirect oxidation ways (see Introduction). The increasing current density would accelerate direct and indirect oxidation reaction. The former accelerated the electron transfer rate between organic contaminants and electrode, while the latter enhanced the generation rate of ·OH as indirect oxidation reagency. ·OH attacks color compounds by adding ·OH to C=C double bond or through the abstraction of hydrogen from aliphatic fractions, which lead to the rapid color reduction [24,25]. The result of this study show a better decolorization efficiency compared to the previous studies treating lignocellulosic ethanol wastewater by aerobic process combined with alum coagulation (89%) [26], photocatalysis (77–91.5%) [27] and ultrafiltration membrane (75%, 98%) [3,28]. In addition, color was rapidly reduced in the first 60 min at the current density of 5 and 10 mA·cm$^{-2}$ with color removal efficiency of 93.6% and 96.1%, respectively; while color was rapidly reduced in the first 30 min at the current density of 20 and 30 mA·cm$^{-2}$ with color removal efficiency of 96.4% and 98.3%, respectively, then slowly reduced. This tendency was also observed during electrochemical decolorization of distillery spent wash [29]. This is likely because of the catalytic selectivity of electrodes during the electrochemical oxidation process [30]: organic contaminants are at first, rapidly oxidized to colorless intermediates, with quick decrement in the current efficiency (Fig. 2b (inset)); and colorless intermediates are further degraded at a slow rate until complete mineralization.

On the other hand, the color-causing compounds of biologically pretreated CEW is closely related to humic substances [14]. This humic substances contain substantial content of aromatic and aliphatic components and relatively smaller content of carboxyl groups [31], of which, the breakdown of conjugated C=C double bond and C=O stretching might be associated with the reduction in color. Similar results had been obtained in melanoidin decoloration by photocatalysis [24].

The evolution of COD was shown as a function of time in Fig. 2b. COD removal substantially increased with increasing current density, resulting to 41.9%, 57.3%, 86.5% and 88.2% of COD removal efficiency within 150 min at current density of 5, 10, 20, and 30 mA·cm$^{-2}$, respectively (Fig. 2b). Compared to the current density of 20 mA·cm$^{-2}$, the COD removal efficiency increment was not obvious (1.7%) at current density of 30 mA·cm$^{-2}$, this was likely because of the unwanted side reaction of oxygen evolution greatly promoted on anode in high current density [9,32], resulting in low current efficiency, and ICE did not increase with increasing current density (from 20 mA·cm$^{-2}$ to 30 mA·cm$^{-2}$) (Fig. 2b (inset)). The removal of COD was relatively lower than that of the color. Similar results have also been observed in electrochemical oxidation treatment of distillery wastewater [13]. Compared to the COD decay, slower DOC removal efficiency at all current densities suggest the formation and accumulation of intermediate organic products. The DOC removal efficiency realized 32.3%, 37.1%, 69.1% and 74.1% within 150 min at current density of 5, 10, 20, and 30 mA·cm$^{-2}$, respectively (Fig. 2c). The decay of DOC was much lower than that of color and COD. Similar results were observed during the degradation of secondary effluent by electrochemical oxidation [33]. This might be due to the incomplete mineralization of color compounds during the electrochemical oxidation process, and the formation of unmineralized products (colorless compounds) could have resulted in the low DOC reduction. Moreover, the COD/DOC ratios at current density of 5, 10, 20, and 30 mA·cm$^{-2}$ decreased as a function of time to 2.06, 1.63, 1.05 and 1.09, respectively, from the initial 2.40, and the low COD/DOC indicated the formation of stable compounds [13].

Increased current density shortens the time required for compliance with National Discharge Standard (GB 27631-2011) (Table 2). However, relatively constant ICE occurs in high current density (Fig. 2b (inset)), because of the unwanted side reaction of oxygen evolution on the anode [9,32]. As a result, the required Es increased with increasing current density, and the corresponding values at current density of 5, 10, 20, and 30 mA·cm$^{-2}$ were 57.1, 87.7, 93.8 and 148.4 kWh kg COD$^{-1}$, respectively (Table 2). In addition, high current density might shorten the life cycle of the electrode. From the above consideration, it can be reasonably suggested that the optimal current density of our study is 20 mA·cm$^{-2}$.

### 3.2. Effect of initial pH

Previous studies have revealed that color-causing compounds of CEW are closely related to humic substances, whose solubility increase with increasing pH, resulting into a darker color [14,34]. In order to better understand the color removal, the effect of the initial pH was investigated at current density of 20 mA·cm$^{-2}$. Fig. 3a shows the removal of color as a function of time at initial pH of 3, 5, 7 and not adjusted 8.9. From the Fig. 3a it can be observed that the initial color was darker with higher pH, and reduced with the decrease of the initial pH. This was likely because pretreated effluent of CEW contains high carbonate alkalinities (4016.5 mg L$^{-1}$) (Table 1), which could scavenge ·OH generated in indirect oxidation and inhibit the ·OH reaction with organic contaminants [35]. As a result, color removal was promoted in the neutral and acidic solution. In addition, COD gradually reduced with decreased initial pH from 8.9 to 5, while it was unfavorable in the acidic solution (pH 3) (Fig. 3b). Similar results were obtained during perfluorooctanoic acid degradation by electrochemical oxidation. Lin et al. [36] associated this phenomenon with the weakening of the electromigration mass transfer, for the pH can affect the existing form of organic contaminants. In the strong acidic condition (pH 3), humic acid colloids were partly or fully

**Table 2**
Reaction time (t) and energy consumption (Es) necessary to meet the National Discharge Standard (GB 27631-2011) under different electrolysis conditions.

| j (mA cm$^{-2}$) | pH | Additives (M) | U (V) | t (h) | Es (kWh kg COD$^{-1}$) |
|---|---|---|---|---|---|
| 5 | 5 | 0.1 | 3.5 | 7.4 | 57.1 |
| 10 | 5 | 0.1 | 4.1 | 4.9 | 87.7 |
| 20 | 5 | 0.1 | 5.1 | 2.1 | 93.8 |
| 30 | 5 | 0.1 | 5.6 | 2.0 | 148.4 |
| 20 | 3 | 0.1 | 5.1 | 2.8 | 125.9 |
| 20 | 5 | 0.1 | 5.1 | 2.1 | 93.8 |
| 20 | 7 | 0.1 | 5.2 | 2.9 | 131.9 |
| 20 | 8.9 (Not adjusted) | 0.1 | 5.1 | 3.4 | 155.2 |
| 20 | 5 | 0 | 7.1 | 2.9 | 183.5 |
| 20 | 5 | 0.01 | 6.9 | 2.6 | 158.8 |
| 20 | 5 | 0.1 | 5.1 | 2.1 | 93.8 |
| 20 | 5 | 0.25 | 5.1 | 2.1 | 94.4 |

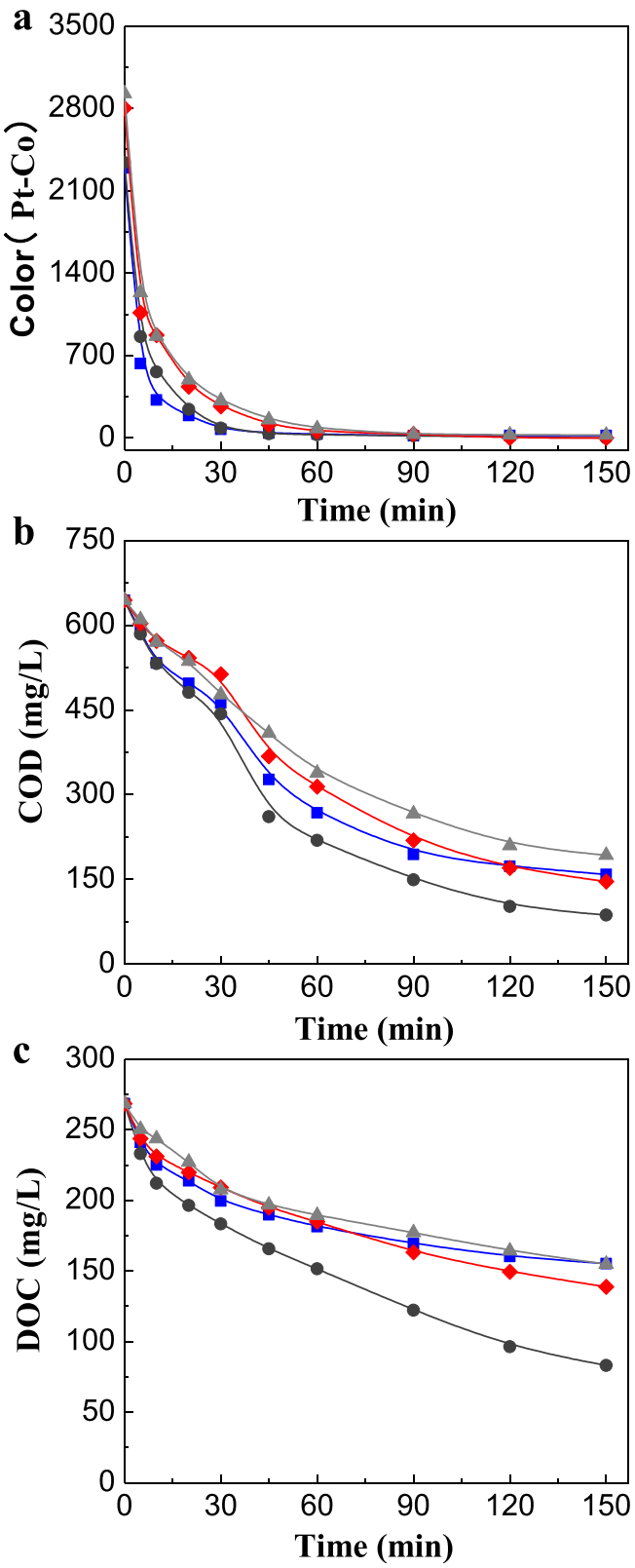


**Fig. 3.** Evolution of Color (a), COD (b) and DOC (c) as a function of time at different initial pH. Electrolysis conditions: solution (200 mL CEW + 0.1 M NaCl) and current density (20 mA·cm$^{-2}$). pH: (■) 3, (●) 5, (◆) 7 and (▲) not adjusted.

undissociated because of the aggregates, chains or networks of humic acid molecules [37]. Faster DOC decay at pH 5 suggests that acidic solution accelerates the removal of organic contaminants. Nevertheless, slower DOC removal efficiency at pH 3 (Fig. 3c) is an indication of the accumulation of more recalcitrant by-products than those formed at other pH [33].

The required Es at the initial pH of 3, 5, 7 and not adjusted 8.9 was 125.9, 93.8, 131.9 and 155.2 kWh kg COD$^{-1}$, respectively (Table 2). These results suggest that the pH 5 was the most suitable before the electrochemical oxidation treatment.

### 3.3. Effect of supporting electrolyte

In chloride-containing solutions, active chlorine species can be formed from anodicoxidation by electrochemical process (Eqs. (5)–(7)) [38], which are responsible for the degradation of organic contaminants. Fig. 4 shows the evolution of color, COD and DOC as a function of time with added supporting electrolyte of NaCl from 0 M to 0.25 M. From the Fig. 4, it can be observed that the color, COD and DOC gradually reduced with the increase of NaCl concentration, and the color completely disappeared after 150 min of electrolysis in supporting electrolyte of 0.1 M and 0.25 M NaCl. It is likely that the high NaCl concentration increased current efficiency for active chlorine formation [39]. However, increasing the concentration of supporting electrolyte could not promote organic contaminants removal. This could possibly be due to competing reactions between ·OH and active chlorine [40], and could also be due to relatively lower oxidation power of active chlorine. These active chlorine species present a lower E° [E°($Cl_2$(aq)/$Cl^-$) = 1.36 V/SHE, E°(HClO/$Cl^-$) = 1.49 V/SHE, E°($ClO^-$/$Cl^-$) = 0.89 V/SHE] than hydroxyl radical [E°(·OH/$H_2O$) = 2.80 V/SHE], however, react homogeneously in the bulk of the solution while the degradation by adsorbed hydroxyl radicals on the anodes is limited by mass transfer [33,41].

$$2Cl^- \rightarrow Cl_2 + 2e^- \quad (5)$$

$$Cl_2 + H_2O \rightarrow H^+ + Cl^- + HClO \quad (6)$$

$$HClO \rightarrow H^+ + OCl^- \quad (7)$$

The high NaCl concentration could increase the conductivity of solution, thereby decreasing the cell voltage and reducing Es (Table 2). The required Es at supporting electrolyte of 0, 0.01, 0.1, 0.25 M NaCl were 183.5, 158.8, 93.8 and 94.4 kWh kg COD$^{-1}$, respectively (Table 2). Since increasing supporting electrolyte continuously could not obviously promote the degradation of organic contaminants, but resulted in a relatively high Es, the most suitable supporting electrolyte was considered as 0.1 M.

From the above results, it can be reasonably concluded that electrochemical oxidation was an effective post treatment of CEW. The required Es met the National Discharge Standard (GB 27631-2011) was 93.8 kWh kg COD$^{-1}$ under the optimal conditions (20 mA·cm$^{-2}$, pH 5 and supporting electrolyte of 0.1 M NaCl). Moreover, optimizing electrochemical cell design can further decrease Es, which exhibit a promising technology in industrial application.

### 3.4. Removal mechanisms of organic contaminants

The efficient electrochemical treatment of CEW might be ascribed to the direct oxidation process on the anode, and indirect oxidation mediated by ·OH, active chlorine (in the presence of chloride) and peroxodisulfate (in the presence of sulfate). Additional experiments were, therefore, conducted in order to investigate the main removal mechanisms of organic contaminants.

Fig. 5 shows the cyclic voltammograms of Sb doped Ti/$SnO_2$ electrode using 0.1 M NaCl as supporting electrolyte. As described in Fig. 5, the current density increased at a potential of approximately +1.0 V in blank solution, which indicated that the

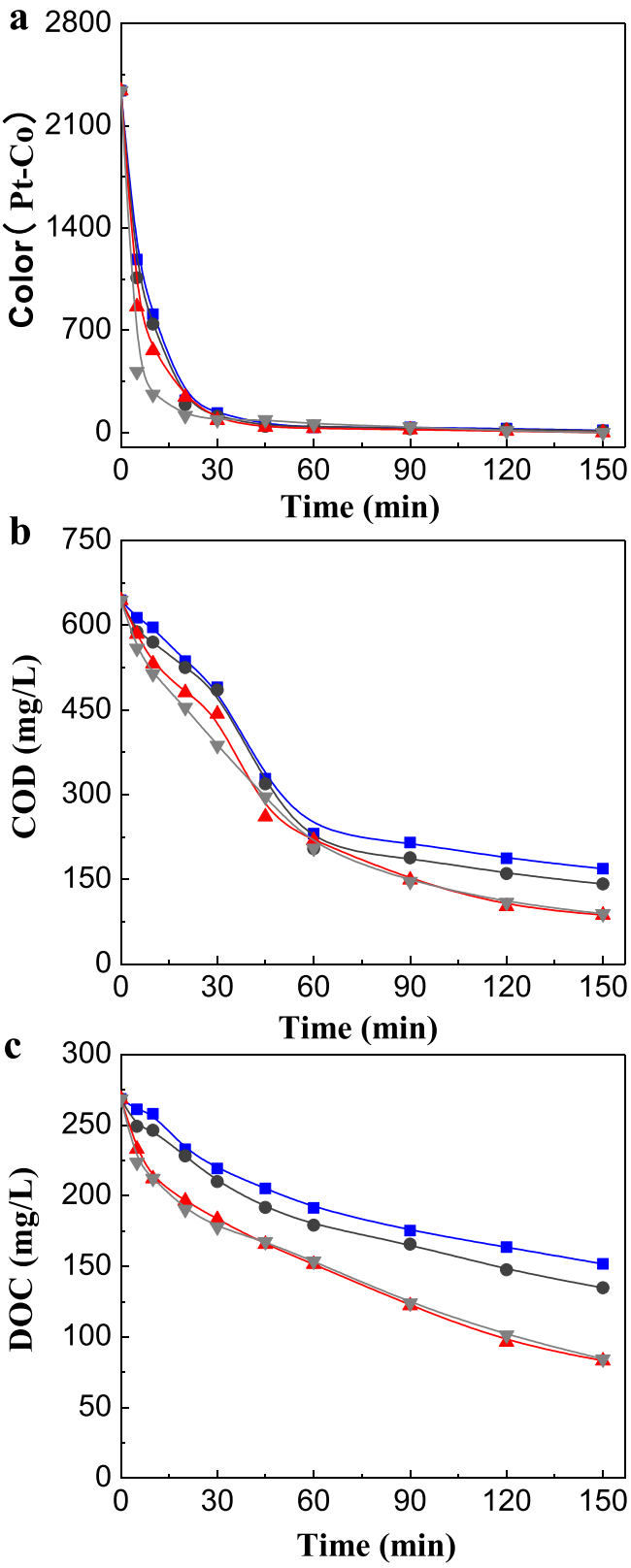


**Fig. 4.** Evolution of Color (a), COD (b) and DOC (c) as a function of time at different supporting media. Electrolysis conditions: solution (200 mL CEW), current density (20 mA·cm$^{-2}$) and pH 5. Additives: (■) 0, (●) 0.01 M, (◆) 0.1 M and (▲) 0.25 M.

electrochemical oxidation of chlorine occurred. However, compared to the blank solution, there was no other clear increase of current density during potential 0 to +2 V, which indicated that direct electrochemical oxidation of biologically pretreated CEW

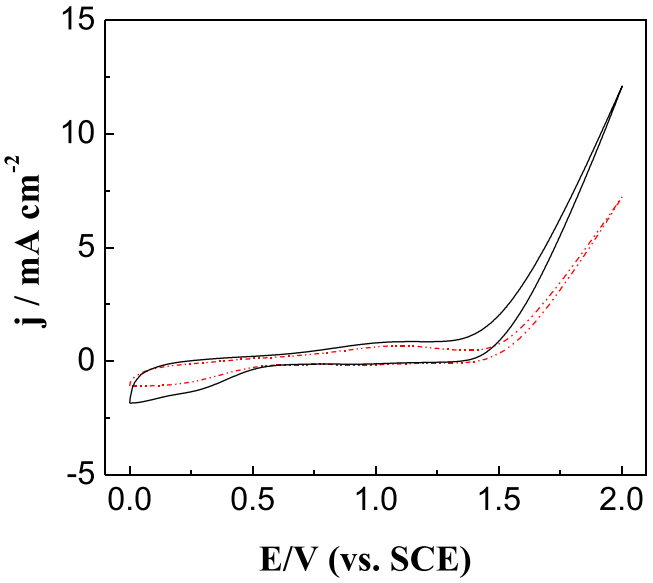


**Fig. 5.** Cyclic voltammograms of biologically treated CEW effluent. Dotted line: blank, 0.1 M NaCl, pH 5.0; solid line: 100 mL biologically treated CEW effluent, pH 5.0.

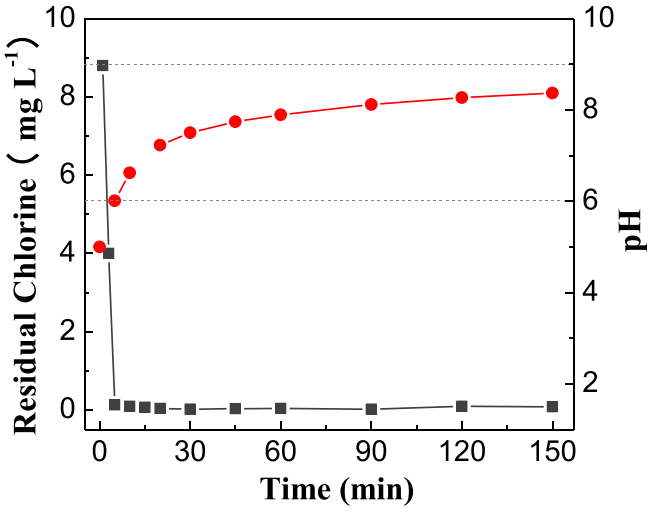


**Fig. 6.** Residual Chlorine and pH as a function of time. Electrolysis conditions: solution (200 mL CEW + 0.1 M NaCl), current density (20 mA·cm$^{-2}$) and initial pH 5.

was not considered. Whereas, the high current densities were observed in the biologically pretreated CEW, this is likely because organic contaminants reacted with adsorbed ·OH discharged from $H_2O$, which facilitated the electron transfer on the anode surface [41].

The efficient degradation capacity of Sb doped Ti/$SnO_2$ electrode might be ascribed to its oxidation mechanism. Sb doped Ti/$SnO_2$ electrode is considered as non-active electrode, which destroys the contaminants mainly by an adsorbed ·OH [8]. This is because that high oxygen potential of this electrode can facilitate organic contaminants reaction with ·OH by restraining the unwanted side reaction of oxygen evolution [42]. Previous studies on the production of ·OH during the electrolysis process by fluorescence spectrum technique, demonstrate that ·OH produced on the surface of Ti/$SnO_2$ electrode was responsible for indirect oxidation of organic contaminants [43]. The possible reactions involve the addition of ·OH to aromatic sites and the abstraction of hydrogen from hydrocarbons, thus resulting in aromatic ring opening and chromophore

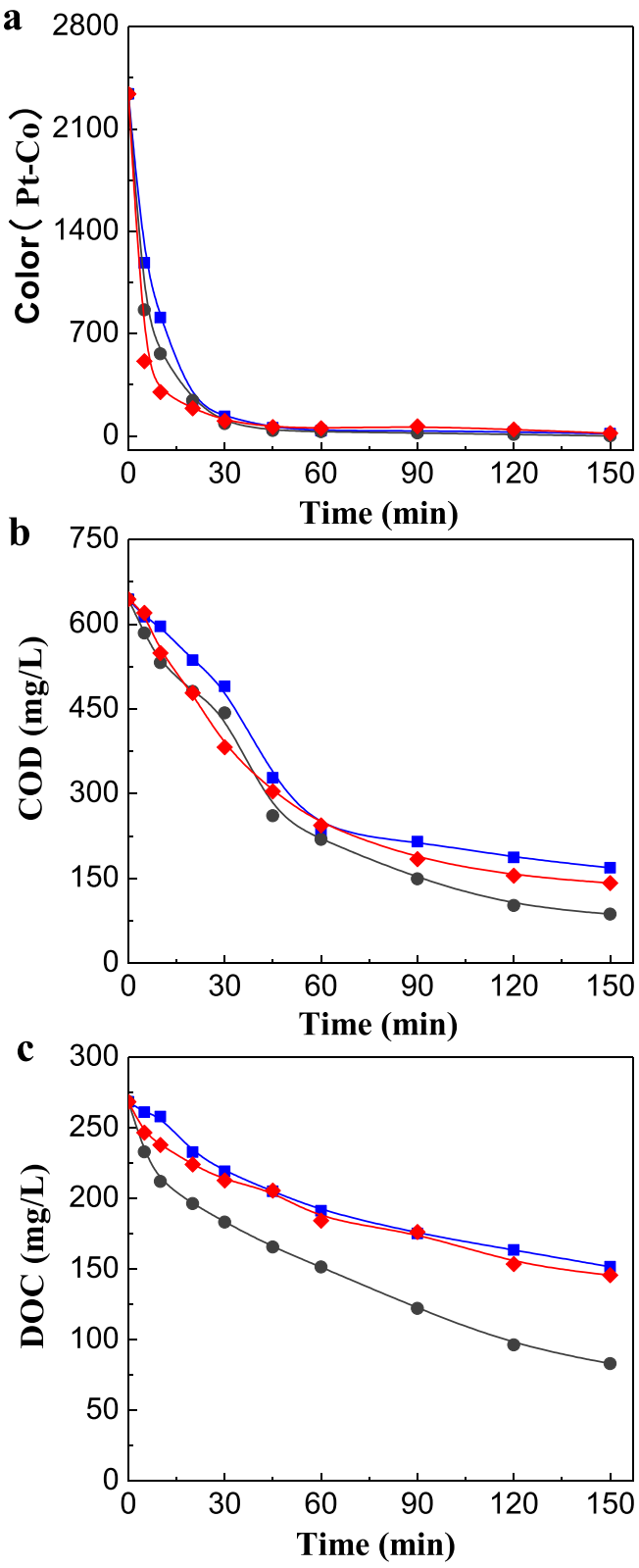


**Fig. 7.** Evolution of Color (a), COD (b) and DOC (c) as a function of time at different supporting media. Electrolysis conditions: solution (200 mL CEW), current density (20 mA·cm$^{-2}$) and pH 5. Additives: (■) 0, (●) 0. 1 M NaCl, (◆) 0.1 M $NaSO_4$.

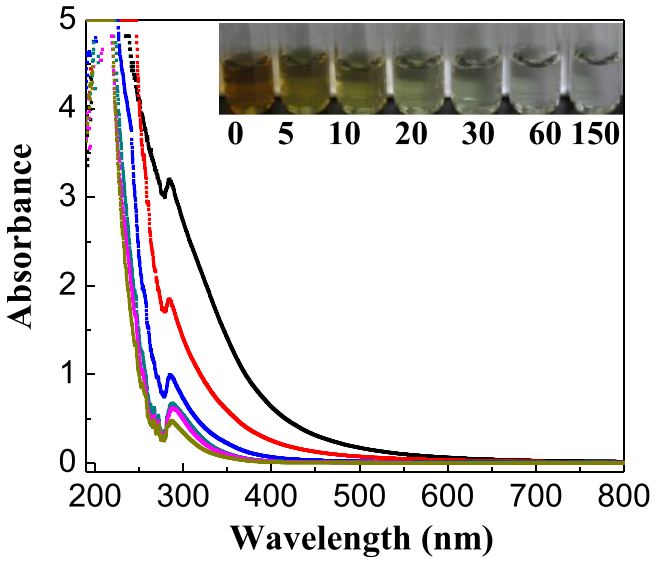


**Fig. 8.** UV–vis spectra of CEW collected as a function of time. Electrolysis conditions: solution (200 mL CEW + 0.1 M NaCl), current density (20 mA·cm$^{-2}$) and pH 5. Time: (■) Initial (double diluted), (●) 10 min, (▲) 30 min, (▼) 60 min, (◆) 90 min, (★) 150 min. Inset: color picture as a a function of time.

groups destruction [24,25]. In a series of electrochemical oxidation processes, the generation of $CO_2$ and the formation of ring-opened products may contribute to a change in the solution pH. The pH of the solution gradually increased during the electrolysis processes (Fig. 6). This was also observed during the degradation of the humic acid by electrochemical oxidation. Motheo et al. [44] associated this phenomenon as compounded by less formation of hydrogen, more oxidation of the organic species and the formation of superficial oxy-hydroxide species.

In the presence of chloride, active chlorine can be formed from anodic oxidation (Eqs. (5)–(7)). To determine the role of these active chlorine, residual chlorine concentration as a function of time was measured. It was detected at the initial period of electrolysis (Fig. 6), while little amount was detected at subsequent time period, which implies that the generated residual chlorine was very rapidly utilized for contaminants degradation. However, the role of active chlorine was weakened by an increase in the pH of the solution during the electrolysis processes. It might be due to the nature of the hypochlorous acid as the main chlorine species at pH < 6; hypochlorous acid and hypochlorite are main chlorine species in the pH range 6–9 [45], where the latter is not expected to be faster due to the lower E°(0.89 V/SHE). Moreover, as described in Fig. 7, COD and DOC removal increased by 12.7% and 25.6%, respectively, compared to that of no supporting electrolyte, while the color removal increased by only 0.5% with the addition of supporting electrolyte of 0.1 M NaCl. These results indicated that the electrogenerated active chlorine played a less important role in organic contaminants removal, while decolorization was negligible.

The biologically pretreated CEW contains sulfate (134.1 mg L$^{-1}$), which can be oxidized to peroxodisulfate during the electrolysis process (Eq. (8)) [23]. Besides, some contaminants could be removed by indirect oxidation through peroxodisulfate. To investigate the role of this oxidant, electrochemical oxidation of CEW using 0.1 M $Na_2SO_4$ as supporting electrolyte was performed. Color removal was promoted at the initial period of supporting electrolyte of 0.1 M $Na_2SO_4$, however, there was no apparent improvement of color removal at a subsequent time period. COD and DOC removal increased by 4.2% and 2.2%, respectively, compared to that of no supporting electrolyte (Fig. 7). The results indicated that the role of electrogenerated oxidant from sulfate was limited in electrochemical treatment of CEW.

$$2SO_4^{2-} \rightarrow S_2O_8^{2-} + 2e^- \quad (8)$$

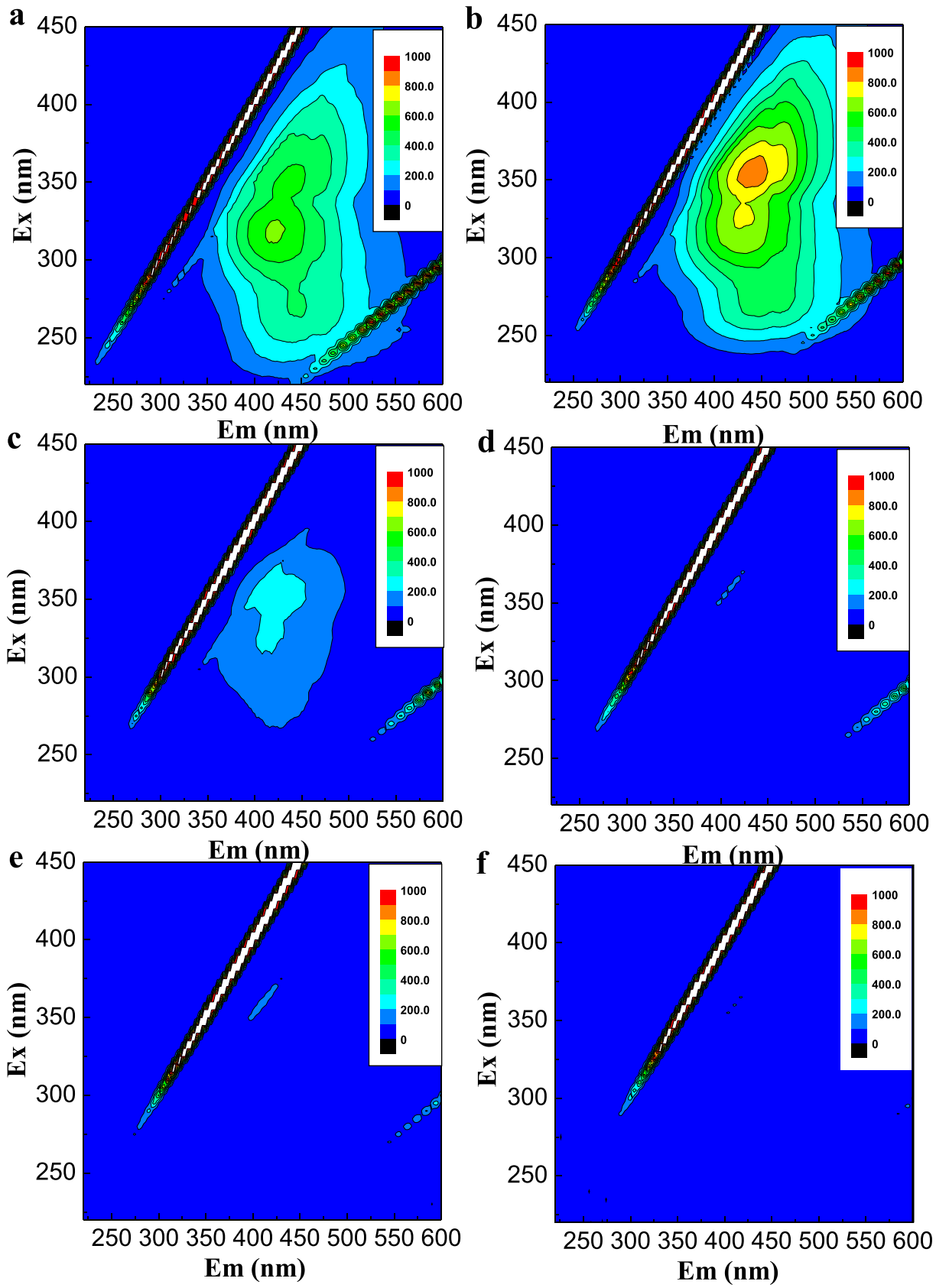


**Fig. 9.** Typical EEM contour of biologically treated CEW: (a) 0 min (1:50 dilution), (b) 10 min (1:10 dilution), (c) 30 min, (d) 60 min, (e) 90 min, (f) 150 min. Electrolysis conditions: solution (200 mL CEW + 0.1 M NaCl), current density (20 mA·cm$^{-2}$) and pH 5.

### 3.5. Decolorization mechanisms of organic contaminants

Electrochemical oxidation biologically pretreated CEW was assessed as a function of time using UV–vis spectra. Fig. 8 exemplifies the behavior observed under the optimal conditions (20 mA·cm$^{-2}$, pH 5 and supporting electrolyte of 0.1 M NaCl). The spectra of CEW at time zero has one main absorption band in the UV region with the maximum at around 280 nm, which was associated with $\pi$–$\pi^*$ electronic transitions of aromatic groups [46]. The absorption band continuously reduced as a function of time due to the =C double bond and C=O stretching decreasing. In addition, the strong absorption band was rapidly reduced in the first 60 min, then slowly reduced. This tendency was in accordance with color and COD removal. It was likely because the COD/DOC continuously decreased from 2.40 to 1.05, implying that the stable colorless compounds were formed. Thus, they were degraded at a slow rate to complete mineralization. The results can also be confirmed by the color change of CEW from Fig. 8 (inset), where the color rapidly reduced and completely disappeared at 150 min of electrolysis time, when complete mineralization had not been achieved.

Moreover, EEM fluorescence spectroscopy could aid in understanding the characteristics of the dissolved organic matter in water and wastewater [47]. For future determination of the decolorization by electrochemical oxidation method, the three-dimensional EEM spectroscopy was applied to characterize the CEW as a function of time under the optimal conditions (20 mA·cm$^{-2}$, pH 5 and supporting electrolyte of 0.1 M NaCl). Each EEM gave spectral information about the chemical compositions of CEW samples (Fig. 9). Shapes of spectra varied as a function of time. Based on the delineated excitation–emission boundaries of dissolved organic matter [47], the peaks identified as humic acid-like peak with different peak intensity were described in all of EEM spectra. One distinctive and intense peak (Ex. 320 nm/Em. 422 nm) was observed in EEM spectra of biologically pretreated CEW. Moreover, two subpeaks (Ex. 270 nm/Em. 450 nm; Ex. 350 nm/Em. 438 nm) correlated with the humic acid-like peak were also observed. Similar multiple-peak distribution was found in paper mill wastewater [48]. These subpeaks might be ascribed to lignin-derived organics during the process of cellulosic ethanol production (Fig. 9a). The intensity of humic acid-like peak decreased as a function of time (Fig. 9b–f). The almost complete disappearance of humic acid-like peak was observed at 60 min indicating that humic substance was reduced, which corresponded to the results of humic acid degradation. On the other hand, the location shift of the humic acid-like peak demonstrated changes in the chemical structure of CEW samples. As shown in Table 3, red shift (towards longer wavelengths) and blue shift (towards shorter wavelengths) were commutative for continuous degradation of CEW. Similar results had been obtained in synthesized wastewater containing humic acid by ozonation [49]. The red shift in this electrochemical process might be ascribed to the addition of hydroxyl group to the structures of humic substance, while the blue shift was correlated with opening of aromatic rings, decrease of conjugation bonds and decrease of $\pi$-electron system [24,25,50]. The possible reactions involve the addition of ·OH to aromatic sites and the abstraction of hydrogen from hydrocarbons, thus resulting in aromatic ring opening and chromophore groups destruction.

**Table 3**
Fluorescence spectral parameters of biologically pretreated CEW samples collected as a function of time.

| Time (min) | Ex/Em | Int.[a] | Ex/Em | Int.[a] | Ex/Em | Int.[a] |
|---|---|---|---|---|---|---|
| 0[b] | 270/450 | 412.8 | 320/422 | 619.9 | 350/438 | 537.0 |
| 10[c] | 275/446 | 456.9 | 325/430 | 722.3 | 350/442 | 860.2 |
| 30 | – | – | 325/416 | 210.1 | 350/422 | 246.0 |
| 60 | – | – | 325/424 | 63.1 | 350/430 | 71.4 |
| 90 | – | – | – | – | 355/404 | 125.1 |
| 150 | – | – | – | – | 370/424 | 97.3 |

[a] Int.: intensity.
[b] 1:50 dilution.
[c] 1:10 dilution.

**Table 4**
The amount of THMs formed during the electrochemical oxidation under the optimal conditions (20 mA·cm$^{-2}$, pH 5 and supporting electrolyte of 0.1 M NaCl) after 150 min.

| Parameter | Unit | CEW |
|---|---|---|
| Chloroform ($CHCl_3$) | μg L$^{-1}$ | 263 |
| Bromodichloromethane ($CHCl_2Br$) | μg L$^{-1}$ | ND |
| Dibromochloromethane ($CHClBr_2$) | μg L$^{-1}$ | ND |
| Bromoform ($CHBr_3$) | μg L$^{-1}$ | ND |
| Total THMs (TTHMs) | μg L$^{-1}$ | 263 |

### 3.6. Generation of organochlorinated by-products

One of the main drawbacks of electrochemical oxidation of organic compounds in the presence of chloride is the formation of organochlorinated by-products [16,17]. Trihalomethanes (THMs) are common and among the most abundant by-products [18,19], which develop in chlorinated water containing organic precursors, such as humic and fulvic acids [20]. Thus, the toxicity of electrochemical treatment of biologically pretreated CEW was assessed by THMs ($CHCl_3$, $BrCHCl_2$, $Br_2CHCl$ and $Br_3CH$) analysis. As presented in Table 4, chloroform was the main THMs detected, with the final total THMs concentration detected as 263 μg L$^{-1}$. Similar results were obtained in landfill leachates [16] and diluted olive pomace leachate [51] degradation by electrochemical oxidation in the presence of NaCl. Considering the formation of oxidation by-products, future investigation for reducing toxicity is needed.

From the above argument, it can be concluded that biologically pretreated CEW was mainly degraded by indirect oxidation through the addition of ·OH to aromatic structures, opening of aromatic rings and destruction of chromophore groups during electrochemical oxidation process. Electrogenerated active chlorine played a less important role in organic contaminants removal, while decolorization was negligible. Direct oxidation and indirect oxidation via peroxodisulfate generated from sulfate oxidation could be negligible.

## 4. Conclusions

The efficient electrochemical treatment of biologically pretreated CEW was achieved. Increase of current density, supporting electrolyte and decrease initial pH could facilitate color and COD removal, and reduce the required Es under the investigated conditions. The excellent performance was mainly ascribed to indirect oxidation mediated by ·OH. In addition, active chlorine formed from chloride oxidation played a less important role in organic contaminants removal. Direct oxidation and indirect oxidation mediated by electrogenerated oxidants from sulfate could be negligible. The formation of chlorination by-products appeared to be low since the final total Trihalomethanes concentration detected was 263 μg L$^{-1}$, with the detection of chloroform as the main Trihalomethanes. Investigation for reducing toxicity of these degradation products is currently underway within our group.

## Acknowledgments

This research was supported by the National Key Research and Development Program of China (2016YFC0401101) and National

Natural Science Foundation of China (51308150, 41405130). The research also got the support from the National Science Technology Pillar Program, China (2015BAD15B0502) and the Heilongjiang Postdoctoral Fund (LBH-Z12132) in China. The author also acknowledge the support from the State Key Laboratory of Urban Water Resource and Environment (2015DX08), and support from the Fundamental Research Funds for the Central Universities (Grant No. HIT.MKSTISP.2016 14).

## References

[1] P. Dwivedi, J.R.R. Alavalapati, P. Lal, Cellulosic ethanol production in the United States: conversion technologies, current production status, economics, and emerging developments, Energy Sustain. Dev. 13 (2009) 174–182.
[2] A.C. Wilkie, K.J. Riedesel, J.M. Owens, Stillage characterization and anaerobic treatment of ethanol stillage from conventional and cellulosic feedstocks, Biomass Bioenergy 19 (2000) 63–102.
[3] A. Luiz, T. Handelsman, G. Barton, H. Coster, J. Kavanagh, Membrane treatment options for wastewater from cellulosic ethanol biorefineries, Desalin. Water Treat. 53 (2015) 1547–1558.
[4] Q. Hu, L. Fan, D. Gao, Pilot-scale investigation on the treatment of cellulosic ethanol biorefinery wastewater, Chem. Eng. J. 309 (2017) 409–416.
[5] D. Pant, A. Adholeya, Biological approaches for treatment of distillery wastewater: a review, Bioresource Technol. 98 (2007) 2321–2334.
[6] Y. Satyawali, M. Balakrishnan, Wastewater treatment in molasses-based alcohol distilleries for COD and color removal: a review, J. Environ. Manage. 86 (2008) 481–497.
[7] S. Mohana, B.K. Acharya, D. Madamwar, Distillery spent wash: treatment technologies and potential applications, J. Hazard. Mater. 163 (2009) 12–25.
[8] D. Miwa, G. Malpass, S. Machado, A. Motheo, Electrochemical degradation of carbaryl on oxide electrodes, Water Res. 40 (2006) 3281–3289.
[9] C.A. Martinez-Huitle, S. Ferro, Electrochemical oxidation of organic pollutants for the wastewater treatment: direct and indirect processes, Chem. Soc. Rev. 35 (2006) 1324–1340.
[10] Y.-J. Feng, Y.-H. Cui, L.-X. Sun, J.-F. Liu, W.-M. Cai, Development of electrochemical technology and high efficiency catalytic electrode for wastewater treatment, J. Harbin Inst. Technol. 4 (2004) 011.
[11] Y. Feng, L. Yang, J. Liu, B.E. Logan, Electrochemical technologies for wastewater treatment and resource reclamation, Environ. Sci. Water Res. Technol. 2 (2016) 800–831.
[12] P. Manisankar, S. Viswanathan, C. Rani, Electrochemical treatment of distillery effluent using catalytic anodes, Green Chem. 5 (2003) 270–274.
[13] P. Piya-areetham, K. Shenchunthichai, M. Hunsom, Application of electrooxidation process for treating concentrated wastewater from distillery industry with a voluminous electrode, Water Res. 40 (2006) 2857–2864.
[14] L. Shan, J. Liu, Y. Yu, J.J. Ambuchi, Y. Feng, Characterization of persistent colors and decolorization of effluent from biologically treated cellulosic ethanol production wastewater, Environ. Sci. Pollut. R (2016) 1–8.
[15] D. Sales, M. Valcárcel, L. Pérez, E. Martinez-Ossa, Activated sludge treatment of wine-distillery wastewaters, J. Chem. Technol. Biotechnol. 40 (1987) 85–99.
[16] A. Anglada, D. Ortiz, A. Urtiaga, I. Ortiz, Electrochemical oxidation of landfill leachates at pilot scale: evaluation of energy needs, Water Sci. Technol. 61 (2010) 2211–2217.
[17] A.Y. Bagastyo, J. Radjenovic, Y. Mu, R.A. Rozendal, D.J. Batstone, K. Rabaey, Electrochemical oxidation of reverse osmosis concentrate on mixed metal oxide (MMO) titanium coated electrodes, Water Res. 45 (2011) 4951–4959.
[18] J.B. Burch, T.M. Everson, R.K. Seth, M.D. Wirth, S. Chatterjee, Trihalomethane exposure and biomonitoring for the liver injury indicator, alanine aminotransferase, in the United States population (NHANES 1999–2006), Sci. Total Environ. 521 (2015) 226–234.
[19] R. López-Roldán, A. Rubalcaba, J. Martin-Alonso, S. González, V. Martí, J.L. Cortina, Assessment of the water chemical quality improvement based on human health risk indexes: Application to a drinking water treatment plant incorporating membrane technologies, Sci. Total Environ. 540 (2016) 334–343.
[20] W.E. Elshorbagy, H. Abu-Qdais, M.K. Elsheamy, Simulation of THM species in water distribution systems, Water Res. 34 (2000) 3431–3439.
[21] J. Lv, Y. Feng, J. Liu, Y. Qu, F. Cui, Comparison of electrocatalytic characterization of boron-doped diamond and $SnO_2$ electrodes, Appl. Surf. Sci. 283 (2013) 900–905.
[22] E. do Vale-Júnior, S. Dosta, I.G. Cano, J.M. Guilemany, S. Garcia-Segura, C.A. Martínez-Huitle, Acid blue 29 decolorization and mineralization by anodic oxidation with a cold gas spray synthesized Sn-Cu-Sb alloy anode, Chemosphere 148 (2016) 47–54.
[23] X. Zhu, J. Ni, P. Lai, Advanced treatment of biologically pretreated coking wastewater by electrochemical oxidation using boron-doped diamond electrodes, Water Res. 43 (2009) 4347–4355.
[24] S. Apollo, M.S. Onyango, A. Ochieng, An integrated anaerobic digestion and UV photocatalytic treatment of distillery wastewater, J. Hazard. Mater. 261 (2013) 435–442.
[25] M. Fukushima, K. Tatsumi, S. Nagao, Degradation characteristics of humic acid during photo-Fenton processes, Environ. Sci. Technol. 35 (2001) 3683–3690.
[26] J. Kavanagh, S. Sritharan, M. Riad, A. Kollaras, Lignocellulosic wastewater treatment, Chemeca 2011: Engineering a Better World, Sydney Hilton Hotel, NSW, Australia, 2011, pp. 1431–1441.
[27] G. RamMohan, T. Goswami, Z. Tian, L. Ingram, P. Pullammanappallil, Photocatalytic treatment for final polishing of wastewater from a cellulosic ethanol process, J. Adv. Oxid. Technol. 16 (2013) 244–251.
[28] T. Handelsman, T. Nguyen, M. Vukas, G. Barton, H. Coster, F. Roddick, J. Kavanagh, Characterisation of foulants in membrane filtration of biorefinery effluents, Desalin. Water Treat. 51 (2013) 1563–1570.
[29] R. Krishna Prasad, S.N. Srivastava, Electrochemical degradation of distillery spent wash using catalytic anode: Factorial design of experiments, Chem. Eng. J. 146 (2009) 22–29.
[30] Y.J. Feng, X.Y. Li, Electro-catalytic oxidation of phenol on several metal-oxide electrodes in aqueous solution, Water Res. 37 (2003) 2399–2407.
[31] A. Koparal, Y. Yildiz, B. Keskinler, N. Demircioglu, Effect of initial pH on the removal of humic substances from wastewater by electrocoagulation, Sep. Purif. Technol. 59 (2008) 175–182.
[32] J. Wei, Y. Feng, X. Sun, J. Liu, L. Zhu, Effectiveness and pathways of electrochemical degradation of pretilachlor herbicides, J. Hazard. Mater. 189 (2011) 84–91.
[33] S. Garcia-Segura, J. Keller, E. Brillas, J. Radjenovic, Removal of organic contaminants from secondary effluent by anodic oxidation with a boron-doped diamond anode as tertiary treatment, J. Hazard. Mater. 283 (2015) 551–557.
[34] H. Kipton, J. Powell, R.M. Town, Solubility and fractionation of humic acid; effect of pH and ionic medium, Anal. Chim. Acta 267 (1992) 47–54.
[35] S.K. Bhargava, J. Tardio, J. Prasad, K. Föger, D.B. Akolekar, S.C. Grocott, Wet oxidation and catalytic wet oxidation, Ind. Eng. Chem. Res. 45 (2006) 1221–1258.
[36] H. Lin, J. Niu, S. Ding, L. Zhang, Electrochemical degradation of perfluorooctanoic acid (PFOA) by Ti/$SnO_2$-Sb, Ti/$SnO_2$-Sb/$PbO_2$ and Ti/$SnO_2$-Sb/$MnO_2$ anodes, Water Res. 46 (2012) 2281–2289.
[37] M. Plaschke, J. Römer, R. Klenze, J. Kim, In situ AFM study of sorbed humic acid colloids at different pH, Colloid Surface A 160 (1999) 269–279.
[38] M. Panizza, G. Cerisola, Electrochemical oxidation as a final treatment of synthetic tannery wastewater, Environ. Sci. Technol. 38 (2004) 5470–5475.
[39] J. Iniesta, J. González-Garcýa, E. Expósito, V. Montiel, A. Aldaz, Influence of chloride ion on electrochemical degradation of phenol in alkaline medium using bismuth doped and pure PbO2 anodes, Water Res. 35 (2001) 3291–3300.
[40] M. Zhou, H. Särkkä, M. Sillanpää, A comparative experimental study on methyl orange degradation by electrochemical oxidation on BDD and MMO electrodes, Sep. Purif. Technol. 78 (2011) 290–297.
[41] L. Xu, Y. Sun, L. Zhang, J. Zhang, F. Wang, Electrochemical oxidation of C.I. Acid Red 73 wastewater using Ti/$SnO_2$-Sb electrodes modified by carbon nanotube, Desalin. Water Treat. 57 (2016) 8815–8825.
[42] X.-Y. Li, Y.-H. Cui, Y.-J. Feng, Z.-M. Xie, J.-D. Gu, Reaction pathways and mechanisms of the electrochemical degradation of phenol on different electrodes, Water Res. 39 (2005) 1972–1981.
[43] H. Ding, Y. Feng, J. Lü, J. Liu, Detection of Hydroxyl Radicals During Electrolysis of Ti/$SnO_2$ Electrode and Analysis of the Electro-catalytic Mechanism, Chinese J. Anal. Chem. 35 (2007) 1395.
[44] A.J. Motheo, L. Pinhedo, Electrochemical degradation of humic acid, Sci. Total Environ. 256 (2000) 67–76.
[45] M. Deborde, U. Von Gunten, Reactions of chlorine with inorganic and organic compounds during water treatment-kinetics and mechanisms: a critical review, Water Res. 42 (2008) 13–51.
[46] C.S. Uyguner, M. Bekbolet, Evaluation of humic acid photocatalytic degradation by UV-vis and fluorescence spectroscopy, Catal. Today 101 (2005) 267–274.
[47] W. Chen, P. Westerhoff, J.A. Leenheer, K. Booksh, Fluorescence excitation - Emission matrix regional integration to quantify spectra for dissolved organic matter, Environ. Sci. Technol. 37 (2003) 5701–5710.
[48] S. Ciputra, A. Antony, R. Phillips, D. Richardson, G. Leslie, Comparison of treatment options for removal of recalcitrant dissolved organic matter, Chemosphere 81 (2010) 86–91.
[49] T. Liu, Z.L. Chen, W.Z. Yu, S.J. You, Characterization of organic membrane foulants in a submerged membrane bioreactor with pre-ozonation using three-dimensional excitation-emission matrix fluorescence spectroscopy, Water Res. 45 (2011) 2111–2121.
[50] J. Swietlik, A. Dabrowska, U. Raczyk-Stanislawiak, J. Nawrocki, Reactivity of natural organic matter fractions with chlorine dioxide and ozone, Water Res. 38 (2004) 547–558.
[51] A. Katsoni, D. Mantzavinos, E. Diamadopoulos, Sequential treatment of diluted olive pomace leachate by digestion in a pilot scale UASB reactor and BDD electrochemical oxidation, Water Res. 57 (2014) 76–86.